

MICROSTRIP-FED MONOPOLE ANTENNA WITH A SHORTED PARASITIC ELEMENT FOR WIDEBAND APPLICATION

C.-F. Tseng

Department of Electronic Engineering
National United University
No. 1 Lien Da, Kung-Ching Li, Miao-Li 36003, Taiwan

C.-L. Huang

Department of Electrical Engineering
National Cheng Kung University
No. 1 University Rd., Tainan 70101, Taiwan

C.-H. Hsu

Department of Electrical Engineering
National United University
No. 1 Lien Da, Kung-Ching Li, Miao-Li 36003, Taiwan

Abstract—A microstrip-fed planar monopole antenna consisting of an inverted-L monopole and a square parasitic element extending directly from ground plane to obtain wideband operation covering Bluetooth/ISM, 2.5 GHz WiMAX, 3.5 GHz WiMAX and 5.2/5.8 GHz WLAN bands is presented. The proposed antenna employs a shorted parasitic element to improve the bandwidth. The return loss of the suggested antenna geometry was calculated by a commercial HFSS 9 simulator and the results are compared with measured return loss, which shows a good agreement between them. Details of the proposed antenna designs and experimental results of the constructed prototypes are presented.

1. INTRODUCTION

A few decades after the earliest investigations of wideband wireless systems, a wide range of applications have been identified. They include ground-penetrating radars, biomedical imaging systems, high-data-rate short-range wireless local networks, communication systems, medium- and long-range radars for military purposes, and others, because of their high spatial and temporal resolution [1]. With advances in wireless systems, the need for broadening frequency bandwidth and sharing multi-frequency bands has increased. Several conventional antennas, such as helical [2], horn [3], monopole [4–6], wide slot [7, 8], and electric-magnetic dipole [9], are also available for wide impedance bandwidth applications. Additionally, multiband resonance can be achieved by adding a parasitic line or a shorted parasitic element to the main monopole patch [10, 11].

Printed antennas with parasitic elements can be used as multiband planar antennas. This investigation presents a design of a printed L-shaped antenna with a parasitic element for operation in Bluetooth/ISM (2400–2484 MHz), 2.5/3.5/5.5 GHz WiMAX (2500–2690/3400–3690/5250–5850 MHz) and 5.2/5.8 GHz WLAN (5150–5350/5725–5825 MHz) bands [12–16]. The square parasitic element is positioned opposite the printed L-shaped radiating element. Introducing the parasitic element provides a significant wideband impedance bandwidth. The performance of the proposed antenna is both calculated and measured.

2. ANTENNA STRUCTURE

As shown in Fig. 1, the proposed antenna can be regarded as an inverted-L monopole, operated as a 0.5 wavelength structure. It is easily fed by a $50\ \Omega$ microstrip line of width $W_1 = 3\ \text{mm}$ in this study. The inverted-L monopole and the microstrip line are printed on the same side of the electric substrate. The FR4 substrate of thickness 1.5 mm, relative permittivity 4.4 and loss tangent 0.0245 are used. In the proposed antenna configuration, the inverted-L monopole can provide the fundamental resonant mode at 2.1 GHz in the absence of the square parasitic element. The antenna can generate the second resonant frequency when the dimension (a) of the square parasitic element plane is properly tuned. This design can remarkably increase the impedance bandwidth. Also a narrow gap separates the square parasitic element from the ground plane. The width of the gap (g) can also affect the resonant frequencies and operating bandwidth. Thus, the width of the gap should also be taken

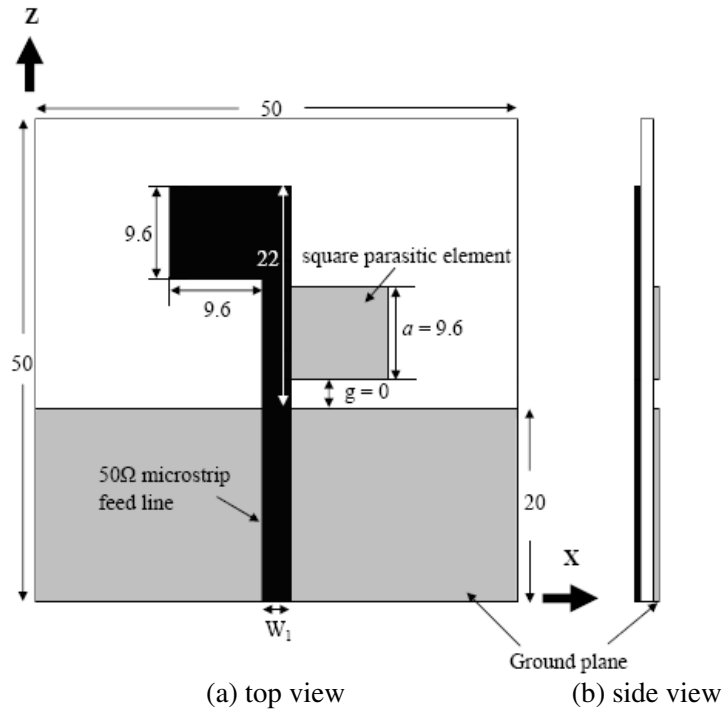


Figure 1. Geometry of the proposed monopole antenna.

into account in determining the proper parameters for the proposed antenna. The proper parameters can be obtained with the aid of the commercially available software, Ansoft High Frequency Structure Simulator (HFSS).

3. EXPERIMENTAL RESULTS AND DISCUSSION

Based on the design presented in Fig. 1, the proposed antenna was constructed and tested. Figure 2 shows the simulated and measured return losses of the proposed antenna with a square parasitic element. The simulated return loss agrees with the measured curve. From the measured data, two resonant modes at about 2.32 and 4 GHz are successfully excited. The -10 dB return loss from 2.12 to over 6 GHz exhibits a bandwidth of more than 95.6% and the Bluetooth/ISM, 2.5/3.5/5.5GHz WiMAX and 5.2/5.8 GHz WLAN bands are covered. Two resonant modes are mainly excited owing to the presence of the inverted-L monopole and square parasitic element, which have lengths

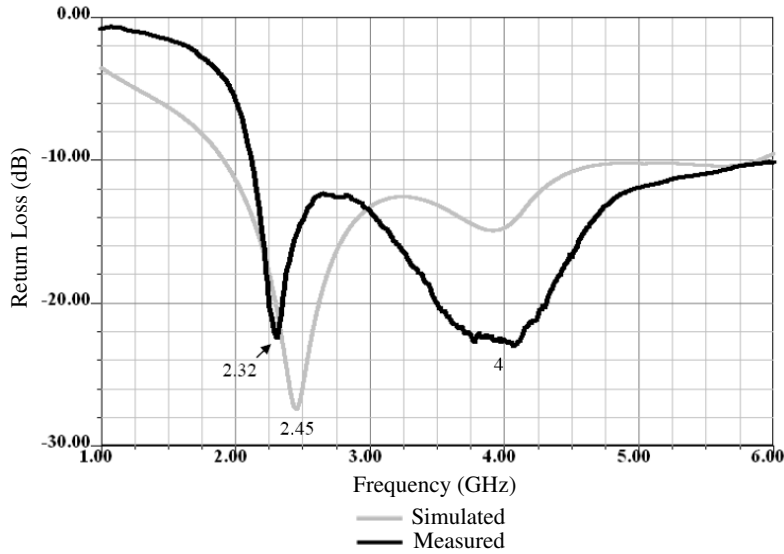


Figure 2. Measured and simulated return loss; $a = 9.6$ mm, $g = 0$ mm.

of about 32 and 19 mm (or about 0.5λ at 2.32 and 4 GHz), respectively.

According to the investigation by Li et al. the configuration of the proposed antenna can be decomposed into radiating mode (unbalanced mode) and balanced mode [17]. Figure 3 displays the calculated unbalanced mode impedance Z_u and the real parts of V/I_u and $V/\alpha I_u$. Additionally, Fig. 4 presents the calculated balanced mode impedance Z_b . As shown in Figs. 3 and 4, the impedance matching around the first resonance is a result of the combination of unbalanced and balanced modes. Moreover, it can be seen that the results in Fig. 4 differ from those in Fig. 3 at the second resonance is introduced at approximately 4 GHz. Hence, the second resonance is determined mainly by the balanced mode. This result is consistent with the previous results on the return loss.

The effects of the parameters a and g on the operation band of the proposed antenna are also studied. Figure 5 plots the simulated return loss as a function of the length (a) of the square parasitic element, as a is varied from 0 to 10 mm. Other parameters are fixed, as given in Fig. 1, while of $g = 0$. When the square parasitic element is not present, the desired upper operation band is also absent. These results clearly indicate that as the length a is increased, the upper mode is shifted to lower frequency. Hence, the upper band of the proposed antenna is formed mainly by the square parasitic element. For $a = 9.6$ mm,

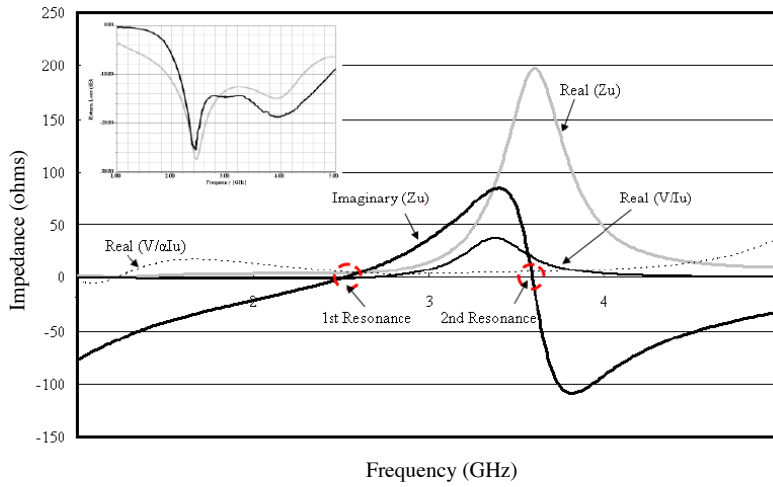


Figure 3. Calculated unbalanced-mode impedance (Z_u) and the real parts of V/I_u and $V/\alpha I_u$ for the proposed antenna.

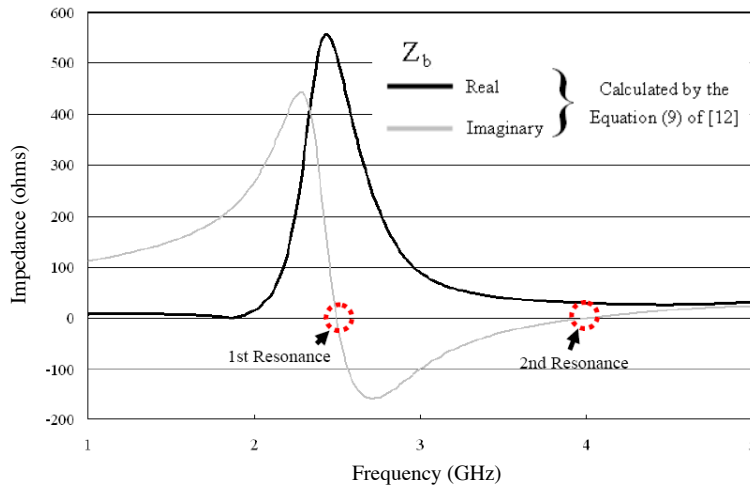


Figure 4. Impedance of the balanced mode (Z_b) calculated using the Equation (9) of [12].

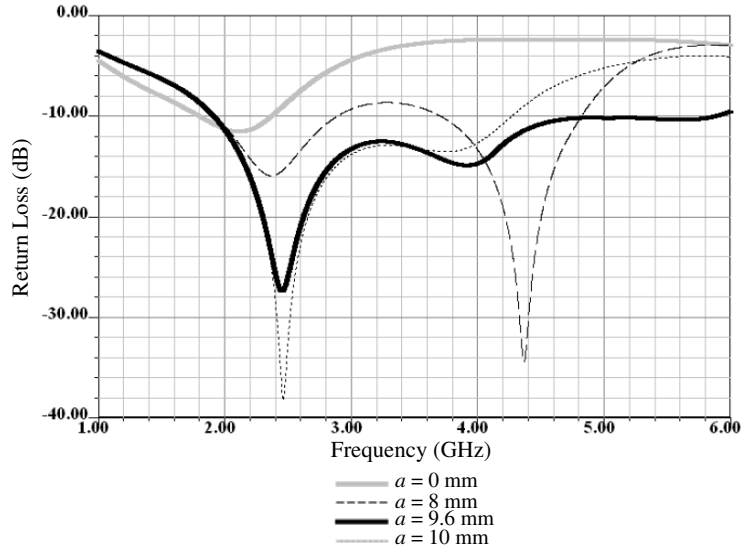


Figure 5. Simulated return loss as a function of the length a of square parasitic element. Other parameters are the same as given in Fig. 1.

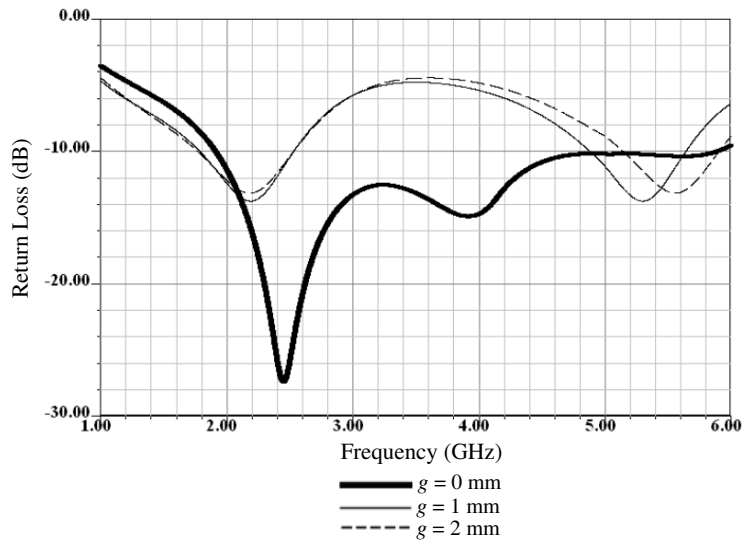


Figure 6. Simulated return loss as a function of the gap g . Other parameters are the same as given in Fig. 1.

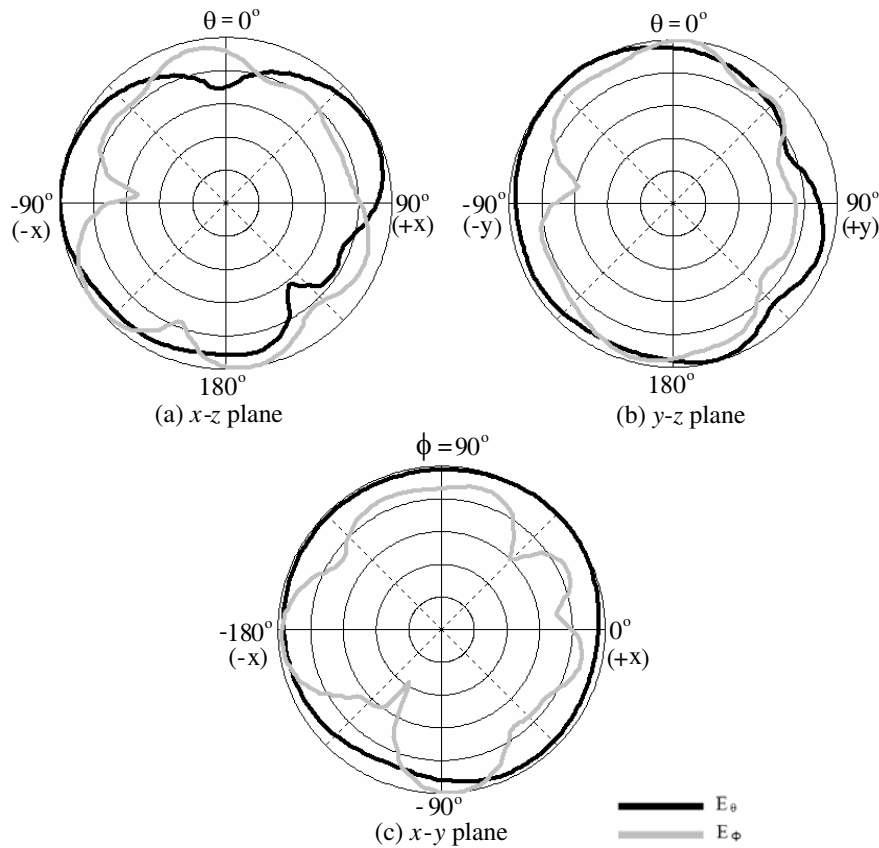


Figure 7. Measured radiation patterns for the proposed antenna at frequency of 2.32 GHz.

the simulated impedance bandwidth, determined from a return loss of -10 dB, reaches 3.98 GHz (1.91–5.89 GHz).

Figure 6 plots simulated return loss as g is varied from 0 to 2 mm. Large effects are seen for the impedance matching of desired dual-resonance excitation. The antenna with $g = 0$ mm outperforms those with $g = 1$ and 2 mm. As shown in Fig. 1, the configuration of the proposed antenna is the same as that of a planar monopole antenna with an irregularly shaped ground plane with $g = 0$ mm. The results obtained as g is increased clearly indicate that the lower resonant mode of the antenna is shifted to lower frequency. On the contrary, the upper resonant mode is shifted to higher frequency. As plotted in Fig. 6, the gap g reduces the impedance matching for the proposed antenna. The

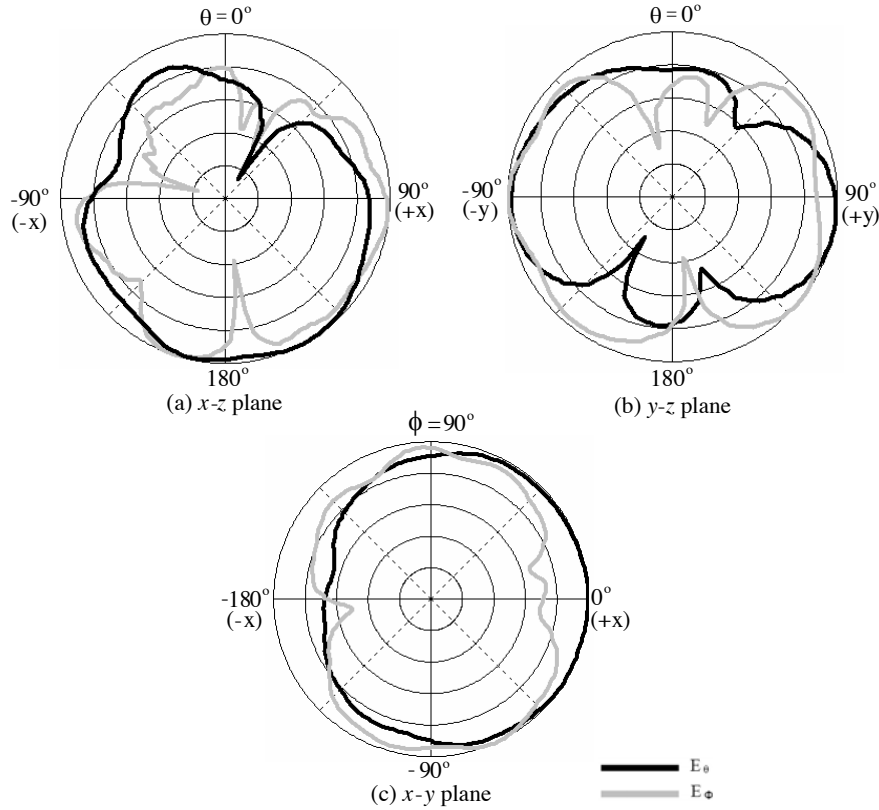


Figure 8. Measured radiation patterns for the proposed antenna at frequency of 4 GHz.

results in Figs. 5 and 6 indicate that the lower and upper resonant frequencies of the antenna can be controlled by adjusting the size and position of the square parasitic element [18].

The radiation characteristics are also investigated. Figure 7 shows the $x-z$, $y-z$ and $x-y$ plane far-field simulated radiation patterns of the proposed antenna at 2.32 and 4 GHz. Figures 8 and 9 plot the measured far-field radiation patterns in the elevation direction ($x-z$ and $y-z$ planes) and the azimuthal direction ($x-y$ plane) at the operating frequencies of 2.32 and 4 GHz for the proposed antenna, respectively. The measurements agree quite closely with the simulated patterns. Monopole-like radiation characteristics with conical patterns in the E -planes ($x-z$ and $y-z$ planes) and an almost omni-directional pattern in the H -plane ($x-y$ plane) are observed. Notably, those in the E -

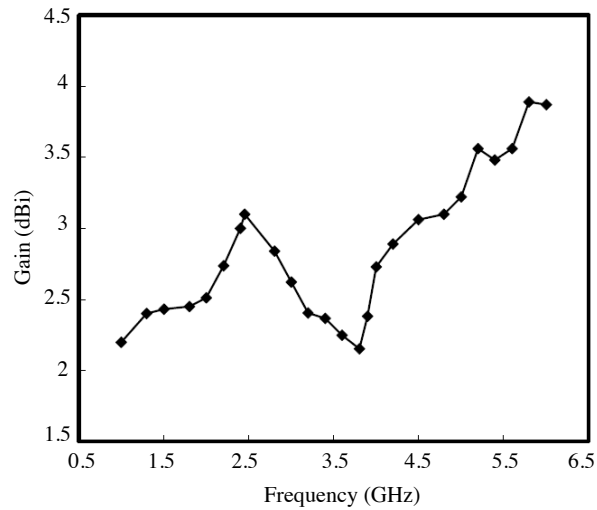


Figure 9. Measured antenna gain for the proposed antenna.

planes (x - z and y - z planes), as expected, are symmetrical with respect to the antenna axis ($\theta = 0$), since the structure of the proposed antenna is symmetrical. This behavior indicates that stable radiation patterns are obtained for the proposed antenna. It is also noted that, measurements at other operating frequencies across the bandwidth of each band yield radiation patterns similar to those plotted. Figure 10 plots the measured antenna gain for frequencies across the operation bands. The antenna gain is from about 2.15 to 3.8 dBi with a gain variation of 1.65 dBi.

4. CONCLUSION

A microstrip-fed monopole antenna with a shorted parasitic element for achieving Bluetooth/ISM, 2.5/3.5 GHz WiMAX and 5.2/5.8 GHz WLAN bands is proposed and studied. The antenna has a simple structure of an inverted-L monopole and a square parasitic element that extends directly from the ground plane. It is easily fabricated at low cost by printing on an FR4 substrate. The square parasitic element is employed for a wideband operation. Good agreement between measured and simulated results is obtained. The radiation patterns are nearly omni-directional over the entire bandwidth with acceptable antenna gain.

REFERENCES

1. Allen, B., M. Dohler, E. E. Okon, W. Q. Malik, A. K. Brown, and D. J. Edwards, *Ultra-wideband Antennas and Propagation*, John Wiley & Sons Inc., New York, 2007.
2. Kraus, J. D. and R. J. Marhefka, *Antennas for All Applications*, John Wiley & Sons Inc., New York, 2002.
3. Balanis, C. A., *Antenna Theory: Analysis and Design*, John Wiley & Sons Inc., New York, 2005.
4. Lau, K.-L., P. Li, and K.-M. Luk, "A monopolar patch antenna with very wide impedance bandwidth," *IEEE Trans. Antennas Propag.*, Vol. 53, No. 2, 655–661, Feb. 2005.
5. Cho, Y. J., K. H. Kim, D. H. Choi, S. S. Lee, and S.-O. Park, "A miniature UWB planar monopole antenna with 5-GHz band-rejection filter and the time-domain characteristics," *IEEE Trans. Antennas Propag.*, Vol. 54, No. 5, 1453–1460, May 2006.
6. Qu, S.-W., C.-L. Ruan, and Q. Xue, "A planar folded ultrawideband antenna with gap-loading," *IEEE Trans. Antennas Propag.*, Vol. 55, No. 1, 216–220, Jan. 2007.
7. Lin, Y.-C. and K.-J. Hung, "Compact ultrawideband rectangular aperture antenna and band-notched designs," *IEEE Trans. Antennas Propag.*, Vol. 54, No. 11, 3075–3081, Nov. 2006.
8. Qu, S.-W., J.-L. Li, J.-X. Chen, and Q. Xue, "Ultrawideband striploded circular slot antenna with improved radiation patterns," *IEEE Trans. Antennas Propag.*, Vol. 55, No. 11, 3348–3353, Nov. 2007.
9. Johnston, R. H., T. C. Choi, and E. Tung, "A compact ultra wide impedance bandwidth antenna," *IEEE AP-S Int. Symp.*, Vol. 2, 1863–1866, 2004.
10. Jan, J. Y. and L. C. Tseng, "Small planar monopole antenna with a shorted parasitic inverted-L wire for wireless communications in the 2.4-, 5.2-, and 5.8-GHz bands," *IEEE Trans. Antennas Propag.*, Vol. 52, 1903–1905, 2004.
11. Huang, C. Y. and P. Y. Chiu, "Dual-band monopole antenna with shorted parasitic element," *Electron. Lett.*, Vol. 41, 1154–1155, 2005.
12. Lin, Y. D. and P. L. Chi, "Tapered bent folded monopole for dual-band wireless local area network (WLAN) systems," *IEEE Antenna Wireless Propag. Lett.*, Vol. 4, 355–357, 2005.
13. Kuo, Y. L. and K.-L. Wong, "Printed double-T monopole antenna for 2.4/5.2 GHz dual-band WLAN operations," *IEEE Trans.*

Antennas Propag., Vol. 51, No. 9, 2187–2192, Sep. 2003.

14. Choi, S. H., J. K. Park, S. K. Kim, and H. Y. S. Kim, “Design of dualband antenna for the ISM band using a backed microstrip line,” *Microw. Opt. Technol. Lett.*, Vol. 41, No. 6, 457–460, Jun. 2004.
15. Deploying License-Exempt WiMAX Solutions Intel Corp. Santa Clara, CA, 2005 [Online]. Available: <http://www.intel.com/netcomms/technologies/wimax>
16. Krishna, D. D., M. Gopikrishna, C. K. Anandan, P. Mohanan, and K. Vasudevan, “CPW-fed koch fractal slot antenna for WLAN/WiMAX applications,” *IEEE Antenna Wireless Propag. Lett.*, Vol. 7, 389–392, 2008.
17. Li, R., B. Pan, J. Laskar, and M. M. Tentzeris, “Analysis of a broadband low-profile two-strip monopole antenna,” *Proc. Int. Symp., Antenna Propagation & EM Theory (ISAPE)*, 1–4, Oct. 2006.
18. Anguera, J., C. Puente, and C. Borja, “A procedure to design stacked microstrip patch antennas based on a simple network model,” *Microwave Opt. Technol. Lett.*, Vol. 30, 149–151, 2001.